Q1

Chemistry, antiproliferative activity and low nephrotoxicity of 3,5-diacetyl-1,2,4-triazol bis(^{4}N-thiosemicarbazone) ligands and their platinum(II) complexes†

Ana I. Matesanz, Céline Joie‡ and Pilar Souza

Received 15th February 2010, Accepted 8th May 2010
First published as an Advance Article on the web ??????
DOI: 10.1039/c003007d

The preparation and characterization of 3,5-diacetyl-1,2,4-triazol bis(4,4-dimethyl thiosemicarbazone) ligand, H_3L^1, and its dinuclear platinum complex $[Pt(\mu\text{-}HL^1)]_2$ is described. The crystal and molecular structure of the platinum complex has been resolved by single crystal X-ray diffraction. The ligands coordinate, in an asymmetric dideprotonate form, to the platinum ions in a tridentate fashion (NNS) and S-bridging bonding modes. Thus the molecular units of the platinum complexes are stacked as dimers. The new compounds synthesized together with the analogous monosubstituted ligand 3,5-diacetyl-1,2,4-triazol bis(4-methylthiosemicarbazone) (H_3L^2) and its dinuclear platinum(II) complex $[Pt(\mu\text{-}H_3L^2)]_2$ have been evaluated for antiproliferative activity *in vitro* against NCI-H460, A2780 and A2780cisR human cancer cell lines. The cytotoxicity data suggest that these compounds may be endowed with important antitumor properties, especially H_3L^1 and $[Pt(\mu\text{-}H_3L^2)]_2$ since they not only circumvent cisplatin resistance in A2780cisR cells but also exhibit high antiproliferative activity in human non-small cell lung cancer NCI-H460 cells. Subsequent nephrotoxic study, in LLC-PK1 cells, show that the four compounds investigated exhibit very low nephrotoxicity with respect to cisplatin.

Introduction

The discovery of cisplatin by Rosenberg, more than three decades ago, was the most important advance in the chemotherapy of human cancer[1] and today this inorganic complex, *cis*-$[PtCl_2(NH_3)_2]$, is one of the most effective drugs employed to treat testicular, ovarian, small cell lung, bladder, cervical and head and neck carcinomas. The main cellular target of cisplatin is assumed to be DNA. The formation of DNA adducts is supposed to cause inhibition of cell growth and finally cell death. However the clinical utility of cisplatin is restricted due to the frequent development of drug resistance, the limited spectrum of tumours against which cisplatin is active and severe normal tissue toxicity being the nephrotoxicity an important side effect which interferes with its therapeutic efficiency.[2-4]

Over the years thousands of cisplatin analogues have been synthesized varying the nature of the leaving groups, the metal or the carrier ligand, yet only a handful of them have been approved for clinical use. The limited success in metal-based anticancer research appears to be caused by the relative lack in structural diversity encountered in the reported compounds. In recent years there has been an emergence of new types of compounds whose structure and mode of action differ from that of cisplatin, especially those that interact with specific molecular targets other than DNA.[5-8]

In this regard, of particular interest are the compounds targeting ribonucleotide reductase (RR), one of the most complex enzymes in the cell, from a biological, structural and regulatory point of view.[9,10]

Increased RR activity has been associated with malignant transformation and tumour cell growth: rapidly proliferating tumours have significant increase in the activity of RR. The correlation between RR activity and tumour growth rate is well established and RR long considered as excellent target for anticancer therapy.[11]

α-(N)-Heterocyclic thiosemicarbazones, (N)-TSCs, have been reported to be among the most effective RR inhibitors yet identified.[12] (N)-TSC compounds are typical tridentate ligands and it has been suggested that they inhibit RR by binding Fe at the active site or that the Fe complex is the active form resulting in destruction of the tyrosyl radical.[13,14]

Many efforts have been devoted to the study of the structure–activity relationship of thiosemicarbazone derivatives.[15-20] It was reported that anticancer activities of the thiosemicarbazones were closely related to the parent aldehyde or ketone group, metal chelation ability and terminal amino substitution. In this sense pyridine-2-carboxaldehyde thiosemicarbazone derivatives have been extensively studied and particularly, the 3-aminopyridine-2-carboxaldehyde thiosemicarbazone (Triapine, Vion Pharmaceuticals, New Haven, CT) is currently being screened for antitumour effect using the National Cancer Institute panel of 60 tumor cell lines and selected for Phase I and II clinical trials.[21-23]

As part of our systematic investigation on the coordination chemistry of thiosemicarbazone derivatives, we recently reported a paper that focused on the structure–antitumor activity

Departamento de Química Inorgánica (Módulo 07), Facultad de Ciencias, c/Francisco Tomás y Valiente n° 7, Universidad Autónoma de Madrid, 28049, Madrid, Spain. E-mail: pilar.souza@uam.es; Fax: (+34)914974833; Tel: (+34)914975156

† CCDC reference numbers 741353 and 763617. For crystallographic data in CIF or other electronic format see DOI: 10.1039/c003007d

‡ Part of the paper includes the direct study presented by this co-author in the Research Project within the Master CHM2295 (Université Catholique de Louvain).

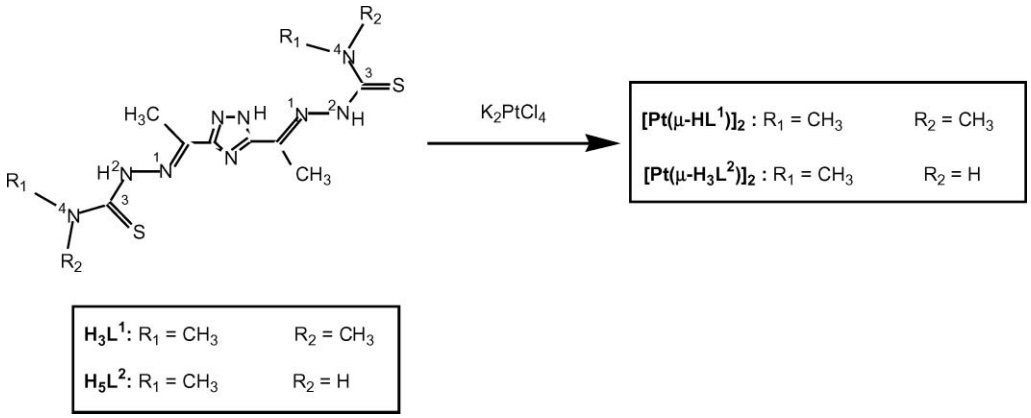

Scheme 1 Ligands and complexes used for the study.

relationships of a series of palladium and platinum α-(N)-heterocyclic bis(4N-monosubstituted thiosemicarbazones) derived from 3,5-diacetyl-1,2,4-triazol.[24] The five-membered heterocycle ring 1,2,4-triazol was selected because it represents a hybrid of pyrazole and imidazole moieties with regard to the arrangement of their three donor atoms, furthermore the additional nitrogen atom in the ring exert an electron-withdrawing effect. In addition, the increased acidity of the ionizable proton facilitates the metal coordination allowing the isolation of dinuclear complexes. The *in vitro* antitumour studies have shown that platinum and palladium complexes exhibit important antiproliferative activity in A2780 and A2780cisR human cancer cell lines, specially the 4N-methyl derivatives displayed the highest activity.

In view of these encouraging results we have extend our studies to 4N,4N-disubstituted derivatives. Thus, this work is aimed to describe the synthesis and chemical characterization of the new 3,5-diacetyl-1,2,4-triazol bis(4,4-dimethyl thiosemicarbazone) ligand, namely H_3L^1, and its dinuclear platinum complex $[Pt(\mu\text{-}H_1L^1)]_2$ (Scheme 1). In order to investigate the influence of 4N-disubstitution on the antitumour activity, the new compounds synthesized together with the related ligand 3,5-diacetyl-1,2,4-triazol bis(4-methylthiosemicarbazone) (H_5L^2) and its dinuclear platinum(II) complex $[Pt(\mu\text{-}H_3L^2)]_2$, previously reported by us,[24,25] have been evaluated for antiproliferative activity *in vitro* against three human cancer cell lines: NCI-H460 (non-small cell lung cancer), A2780 and A2780*cis*R (epithelian ovarian cancer). Nephrotoxicity studies, on normal human renal LLC-PK1 cells, have been also carried out as an attempt to provide an insight into the pharmacological properties of these compounds. The single-crystal X-ray structures of $[Pt(\mu\text{-}HL^1)]_2$ and H_5L^2 are also discussed.

Results and discussion

Synthesis and spectroscopic characterization

Two new 4N-disubstituted bis(thiosemicarbazone) compounds, H_3L^1 and $[Pt(\mu\text{-}HL^1)]_2$, have been synthesized with high purities and acceptable yields. The compounds obtained are stable to air and moisture and were characterized by elemental analysis, FAB^+ spectrometry and IR and ^1H NMR spectroscopy. The complex is a neutral non-conducting compound and analytical results are consistent with the formation of the neutral dimeric species since the FAB^+ mass spectrum of the complex shows a peak at m/z 1097.2 for $[\{Pt(\mu\text{-}HL^1)\}_2 + H]^+$ and the isotopic patterns of this signal fit well with the theoretical isotopic distributions.

The significant IR vibrational bands and the ^1H chemical shift values of the free ligand and its platinum(II) complex are listed in the Experimental section and Scheme 1 shows the numbered structure of the free ligand. Comparison of the IR spectrum of the complex with that of the free ligand shows the expected differences given the dideprotonation and coordination shown by the X-ray study. The υ(NH-triazol) disappears in the spectrum of the platinum complex as a consequence of the deprotonation of the triazole ring and the υ(C=S) thioamide IV band shifts to lower wavenumbers (790 cm^{-1}) indicating coordination *via* the thioamide sulfur atom. However, coordination only induces minor changes in υ(C=N).

The ^1H NMR spectrum of H_3L^1 shows a singlet, integrating as one hydrogen, at $\delta = 14.9$ ppm which is assigned to the triazolic proton. Other two singlets integrating as one hydrogen, at $\delta =$ 13.0 and 9.9 ppm are assigned to the protons attached to the ^2N atoms, the downfield shift of one of these protons is probably due to its participation in intra- or intermolecular hydrogen bonding interactions since the hydrogen bonding decreases the electron density around the proton and thus moves the proton absorption to a lower field.[26] Finally, the singlets at 3.3, 3.2 and 2.3 ppm are assigned to the CH_3 protons of the 4N atoms and triazole moiety respectively.

For $[Pt(\mu\text{-}H_1L^1)]_2$, ^1H NMR integrations and signal multiplicities are in agreement with the proposed structure, so the signal assigned to the triazole proton, in the spectrum of the H_3L^1 ligand, do not appear and only one $-^2NH-$ resonance is shown. The X-ray structure of the complex reveals the existence of an intramolecular hydrogen bonding $^2N-H{=}N$(triazol) in agreement with the ^1H NMR assignments.

Description of the crystal structures

Good quality crystals suitable for single crystal X-ray diffraction analysis were obtained for $[Pt(\mu\text{-}H_1L^1)]_2$ and H_5L^2 compounds by recrystallization in dimethylsulfoxide (DMSO).

The molecular structure of free ligand H_5L^2, which crystallized with two DMSO molecules, together with the atomic numbering

Table 1 Crystal data and structure refinement for H_5L^2 and $[Pt(\mu\text{-}HL^1)]_2$ compounds

	H_5L^2	$[Pt(\mu\text{-}HL^1)]_2$
Formula	$C_{14}H_{29}N_9O_2S_4$	$C_{24}H_{38}N_{18}OPt_2S_4$
Molecular weight	483.70	1113.14
Crystal system	Monoclinic	Monoclinic
Space group	$P2_1/n$	$P2/n$
a/Å	12.5254(7)	8.1428(7)
b/Å	11.4690(6)	12.4059(10)
c/Å	17.0475(9)	19.2779(18)
α/°	90	90
β/°	108.249(2)	96.615(4)
γ/°	90	90
V/Å^3	2325.8(2)	1934.5(3)
λ(Mo-Kα)/Å	0.71073	0.71073
T/K	100(2)	296(2)
Z	4	2
D_c/g cm^{-3}	1.381	1.911
F(000)	1024	1072
μ/mm^{-1}	0.438	7.487
Independent reflections	6025 [R(int) = 0.0384]	5654 [R(int) = 0.0402]
Observed reflections	85 578	54 344
Final R indices [$I > 2\sigma(I)$]	$R_1 = 0.0448$, w$R_2 = 0.1239$	$R_1 = 0.0349$, w$R_2 = 0.0904$
R indices (all data)	$R_1 = 0.0565$, w$R_2 = 0.1354$	$R_1 = 0.0588$, w$R_2 = 0.1172$
Goodness of fit on F^2	1.079	1.221

Table 2 Selected bond distances (Å) and angles (°) for H_5L^2 and $[Pt(\mu\text{-}HL^1)]_2$ complex

H_5L^2		$[Pt(\mu\text{-}HL^1)]_2$			
S(1)–C(2)	1.684(2)	S(1)–C(1)	1.813(8)	N(3)–Pt(1)–N(4)	80.0(2)
S(2)–C(9)	1.678(2)	S(2)–C(10)	1.721(6)	N(3)–Pt(1)–S(1)	84.50(16)
C(2)–N(1)	1.325(3)	C(1)–N(1)	1.345(9)	N(3)–Pt(1)–S(2)	176.26(15)
C(2)–N(2)	1.369(3)	C(1)–N(2)	1.271(9)	N(4)–Pt(1)–S(1)	164.48(14)
C(3)–N(3)	1.288(3)	C(2)–N(3)	1.283(8)	N(4)–Pt(1)–S(2)	103.74(14)
C(7)–N(7)	1.290(2)	N(2)–N(3)	1.371(7)	S(1)–Pt(1)–S(2)	91.76(7)
C(9)–N(8)	1.376(3)	Pt(1)–S(1)	2.2532(17)		
C(9)–N(9)	1.320(3)	Pt(1)–S(2)	2.2892(16)		
N(2)–N(3)	1.364(2)	Pt(1)–N(3)	2.016(5)		
N(7)–N(8)	1.361(2)	Pt(1)–N(4)	2.047(5)		

scheme is shown in Fig. 1. Crystallographic data is shown in Table 1 with selected bond lengths shown in Table 2.

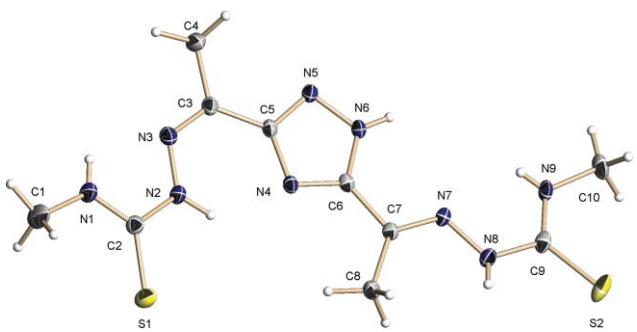

Fig. 1 Molecular structure of H_5L^2 ligand.

The sulfur atom S(1) and the azomethine nitrogen atom N(3) are in *trans* position with respect to the C(2)–N(2) bond and the same configuration is observed for S(2) and N(7) with respect to the C(9)–N(8) bond, therefore the ligand exists in *E* configuration which is often observed in thiosemicarbazones.[27] The azomethine bond distances of 1.288(3) and 1.290(2) are in conformity with a formal C=N double bond and the C–S bond distances of 1.678(2) and 1.684(2) Å, are very close to a formal C=S double bond length, these facts confirm the existence of the thiosemicarbazone groups in the thione form, in the solid state.[28] However, the N(3)–N(2), N(2)–C(2) and N(7)–N(8), N(8)–C(9) bond distances are intermediate between the ideal values of corresponding single and double bonds which is indicative of some electron delocalization along the thiosemicarbazide side chains.

The whole molecule is almost planar and the presence of the intramolecular N(2)–H···N(4) hydrogen bond, reinforces this planarity. The remaining N–H groups form intermolecular hydrogen bonds with oxygen atoms from the DMSO solvent molecules. The extended hydrogen bonding network formed drives the crystal packing.

The molecular structure of platinum complex $[Pt(\mu\text{-}H_1L^1)]_2$ together with the atomic numbering scheme is shown in Fig. 2. Crystallographic data is shown in Table 1 with selected bond lengths shown in Table 2.

The crystallographic analysis reveals that each unit consists of a discrete molecule of complex $[Pt(\mu\text{-}H_1L^1)]_2$ and one free lattice water molecule (the H atoms of the water molecule were not located in the Fourier difference map). This neutral Pt(II) dinuclear compound crystallizes in the monoclinic $P2/n$ space group with $Z = 2$ and its crystallographic analysis reveals

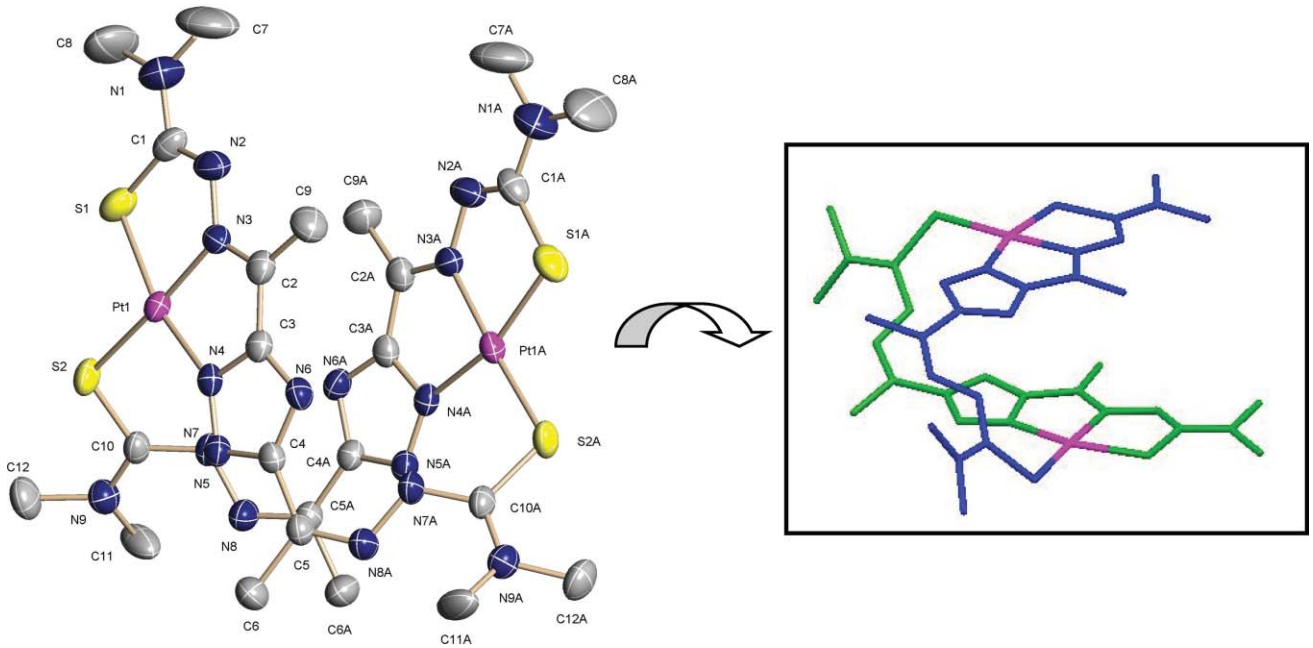

Fig. 2 Left: molecular structure of platinum complex $[Pt(\mu\text{-}HL^1)]_2$ (hydrogen atoms are omitted for clarity). Right: Capped sticks representation of the complex.

unambiguously a dimeric structure which results from the pairing of two mononuclear subunits through two thiosemicarbazone moieties bridges.[29] The electroneutrality of the compound needs the H_3L^1 ligand to lose two protons. As expected, the N(3)–H and N(2A)–H are lost and, consequently, they have not been detected from the difference Fourier maps.

Each Pt(II) center is four coordinated with a [NNSS] donor environment, *via*: one triazolic nitrogen atom, the iminic nitrogen and sulfur atoms belong to the deprotonated arm of one ligand molecule, and being the fourth position occupied by a sulfur atom of the non deprotonated arm from the other ligand. Thus, the deprotonated thiosemicarbazone arm behaves as a bidentate and the neutral one behaves as monodentate acting as a bridge (see Fig. 2).

The Pt–N [2.016(5), 2.047(5) Å] and Pt–S [2.2532(17), 2.2892(16) Å] bond distances are comparable with those reported for Pt(II) thiosemicarbazone complexes.[30,31] A careful examination of these bond length data shows that the Pt–N_{iminic} distance is shorter than Pt–$N_{triazolic}$ indicating stronger coordination of the platinum center to the imine nitrogen and this feature is common to previously studied platinum(II) complexes,[24] as well as other transition metal complexes[32-34] of heterocyclic TSCs. Moreover, the bond length Pd–S to the non-bridging sulfur atom is shorter than Pd–S bridging sulfur atom, and as expected.

The bond angle data indicate that the stereochemistry around each platinum(II) ion is almost planar. The angles deviate slightly from that expected for a regular square-planar geometry, this distortion may be attributed to the restricted bite angle of the tridentate moieties. The coordination results in the formation of two five membered (PdSCNN and PdNCCN) chelate rings for each platinum(II) ion, which are coplanar with the deprotonated triazole ring.

It is important to note that upon coordination, the deprotonated arm undergoes significant evolution from the thione to the thiol form, C–S distance of 1.813(8), while the neutral thiosemicarbazone arm present a shorter C–S bond length of 1.721(6). The C–N and N–N bond distances are intermediate between formal single and double bonds, pointing to extensive delocalization over the entire 3,5-diacetyl-1,2,4-triazole bis(thiosemicarbazone) skeleton.

Interestingly, the flexibility of the ligand originating from the free rotation of the two thiosemicarbazone arms around the C(2)–C(3) and C(4)–C(5) single bonds, allows the ligand to ligate the two metal ions in a twist conformation generating two parallel coordination planes.[35] Particularly, between the two triazole moieties, the interplane separation being 3.27 Å is considered optimal for π–π interactions (intramolecular stacking). This arrangement is reinforced by intramolecular hydrogen bonds between the ^{2}NH of the bridging thiosemicarbazone moieties and uncoordinated triazole nitrogen atoms [N(7)–H(7) ··· N(6) 2.755(7) Å].

It is suggested that water molecules link the adjacent dimeric units *via* intermolecular hydrogen bonds involving the remaining uncoordinated triazole nitrogen atoms with distances of ~2.9 Å which are in the range of moderate-strength hydrogen bonds.[36] The crystal lattice is further stabilized by intermolecular π–π stacking interactions between successive thiosemicarbazone moieties (3.76 Å).

Antiproliferative activity in human NCI-H460, A2780 and A2780cisR cell lines

To analyze the potential of the compounds as antitumour agents, the new compounds synthesized together with 3,5-diacetyl-1,2,4-triazol bis(4-methylthiosemicarbazone) (H_5L^2) and its platinum(II) complex $[Pt(\mu\text{-}H_3L^2)]_2$ were tested (in powder solid form) for their antiproliferative activity *in vitro* against the human cancer cell lines: NCI-H460 (non-small cell lung cancer), A2780 and

Table 3 *In vitro* antiproliferative activity of the bis(thiosemicarbazone) compounds and cisplatin, evaluated in human NCI-H460 (non-small lung cancer), A2780 and A2780cisR (epithelian ovarian cancer) cell lines

	A2780		A2780cisR			NCI-H460	
	%Inhibition (100 μM)	IC_{50}/μM	%Inhibition (100 μM)	IC_{50}/μM	RF[a]	%Inhibition (100 μM)	IC_{50}/μM
H_3L^1	82 ± 1	18 ± 3	85 ± 2	22 ± 1	(1.2)	53 ± 2	32 ± 3
$[Pt(\mu\text{-}HL^1)]_2$	90 ± 1	10 ± 1	91 ± 2	18 ± 1	(1.8)	30 ± 4	>100
H_5L^2	77 ± 4	39 ± 2	40 ± 4	>100	—	30 ± 3	>100
$[Pt(\mu\text{-}H_3L^2)]_2$	88 ± 2	40 ± 2	88 ± 4	56 ± 3	(1.4)	92 ± 1	53 ± 2
Cisplatin	93 ± 3	0.44 ± 0.04	93 ± 3	4.7 ± 0.3	(10.7)	87 ± 2	4.5 ± 0.2

[a] RF, resistance factor (*n*-fold) in parentheses. The fold resistance equals the IC_{50} of the resistant cell divided by the IC_{50} of the parental cells.

Q2 A2780cisR (ephileian ovarian cancer). For comparison purposes the cytotoxicity of cisplatin was evaluated under the same experimental conditions.

Table 3 shows that the ^{4}N,^{4}N-disubstituted H_3L^1 molecule presents important antiproliferative activity in both A2780, cisplatin sensitive, and A2780cisR, cisplatin resistant cell lines. Of particular relevance is the value of the resistance factor, RF: IC_{50}(A2780cisR)/IC_{50}(A2780), which is indicative of activity against the cisplatin resistant cell line. However the ^{4}N-monosubstituted H_5L^2 molecule, active in A2780 cells, does not retain the activity in A2780cisR. The H_3L^1 molecule also exhibits antiproliferative activity in NCI-H460 cell line with an IC_{50} value in the low-micromolar range, while the H_5L^2 molecule remains inactive at concentration 100 μM. Analysis of the data indicates that the inhibitory potency, in the two molecules tested, increases with the presence the two methyl groups attached to the ^{4}N atom. Thus, from the chemical point of view, the greater terminal steric bulk could result in greater endogenous metal coordination efficiency although other mechanisms of action may be involved.

Upon complexation, the most cytotoxic compound H_3L^1 led to dinuclear platinum complex $[Pt(\mu\text{-}H_1L^1)]_2$ which showed to be a slightly higher potent than the parent ligand in A2780 and A2780cisR cell lines but in NCI-H460 cell line becomes inactive at concentration 100 μM.

However compound H_5L^2 enhances their activity upon the complexation, thus the resulting dinuclear platinum $[Pt(\mu\text{-}H_3L^2)]_2$ complex presents important antiproliferative activity in the three cell lines tested. The cytotoxicity data against A2780 and A2780cisR cell lines indicate that this platinum complex is able to circumvent cisplatin resistance. Because the activity of this dinuclear complex is higher than that the parent (N)-TSC ligand it is most likely that part of the biochemical mechanism of action may be not only due to the inhibition of RR but both the metal and the ligand determine the biological activity. Indeed, these compounds could act through dual or even multiple mechanisms of action including covalent and non-covalent interactions with DNA such hydrogen bonding, electrostatic interactions and intercalation.

Nephrotoxicity

In order to investigate possible adverse side effects that may occur such nephrotoxicity, the compounds were subsequently tested (in powder solid form) *in vitro* on normal human renal LLC-PK1 cells. For comparison purposes the toxicity of cisplatin was evaluated under the same experimental conditions.

Table 4 *In vitro* antiproliferative activity of the bis(thiosemicarbazone) compounds and cisplatin, evaluated in normal human LLC-PK1 renal cells

	LLC-PK1	
	%Inhibition (100 μM)	IC_{50}/μM
H_3L^1	40 ± 5	> 100
$[Pt(\mu\text{-}HL^1)]_2$	91 ± 2	20 ± 1
H_5L^2	4 ± 2	> 100
$[Pt(\mu\text{-}H_3L^2)]_2$	7 ± 3	> 100
Cisplatin	92 ± 1	7.03 ± 0.08

As Table 4 shows, the H_3L^1, H_5L^2 and $[Pt(\mu\text{-}H_3L^2)]_2$ compounds show, at 100 μM concentration, very low cellular growth inhibition (< 50%) and therefore had not evaluable cytotoxicity (IC_{50} > 100 μM).

The complex $[Pt(\mu\text{-}H_1L^1)]_2$ and cisplatin presented, at 100 μM concentration, a cellular growth inhibition > 50% and their inhibitory potential (IC_{50}) was measured by calculating concentration-percentage inhibition curves.

Experimental

Measurements

Elemental analyses were performed on a LECO CHNS-932 microanalyzer. Fast atom bombardment (FAB) mass spectra were performed on a VG AutoSpec spectrometer (nitrobenzyl alcohol matrix). ^{1}H NMR spectra (DMSO-d_6) were recorded on BRUKER AMX-300 spectrometer. Infrared spectra (KBr pellets) were recorded on a Bomen-Michelson spectrophotometer (4000–400 cm^{-1}).

Materials

Solvents were purified and dried according to standard procedures. Hydrazine hydrate, L-lactic acid, 4-methylthiosemicarbazide, 4,4-dimethylthiosemicarbazide and potassium tetrachloridoplatinate(II) were commercially available from Aldrich.

Synthesis of compounds

3,5-Diacetyl-1,2,4-triazol bis(4,4-dimethylthiosemicarbazone) ligand, H_3L^1. It was prepared by reacting ethanolic solutions of 4,4-dimethylthiosemicarbazide (0.238 g, 2 mmol) and 3,5-diacetyl-1,2,4-triazol (0.153 g, 1 mmol) which were prepared as described in the literature.[37] The reaction mixture was heated

under reflux for 5 h and then was left to stand to ambient temperature. The pale yellow solid formed was filtered and washed with cold ethanol and diethyl ether and dried *in vacuo*. Yield (54%), mp 181 °C. Elemental analysis found, C, 38.60; H, 6.40, N, 31.55; S 15.80; $C_{12}H_{21}N_9S_2 \cdot MeOH \cdot H_2O$ requires C, 38.50; H, 6.70, N, 31.10; S 15.80%. MS (FAB$^+$ with *m*NBA matrix) *m*/*z* 356.1 (68%) for $[C_{12}H_{21}N_9S_2+H]^+$. IR (KBr pellet): ν/cm^{-1} 3361 (s, NH-triazol), 3217 and 3044 (w, ^{2}NH), 2923 (s, CH), 1595 (s, CN), 799 (w, CS-thioamide IV band). ^{1}H NMR (100 MHz, DMSO-d_6): δ (ppm) 14.99 (s, NH-triazol), 13.08 and 9.97 (s, ^{2}NH), 3.27 and 3.16 (s, CH_3-thiosemicarbazide), 2.37 (s, CH_3-triazol).

[Pt(μ-HL^1)]$_2$ platinum(II) complex. It was obtained by reacting a methanol (20 mL) suspension of the 3,5-diacetyl-1,2,4-triazol bis(4,4-dimethylthiosemicarbazone) ligand with a water solution (5 mL) of potassium tetrachloridoplatinate(II). The reaction mixture was stirred for 15 h at room temperature. The resulting orange solid obtained was filtered, washed with methanol and diethyl ether and dried *in vacuo*. Yield (52%), mp 277 °C (decomposes). Elemental analysis found, C, 20.70; H, 4.25, N, 18.75; S 9.15; $C_{24}H_{38}N_{18}S_4Pt_2 \cdot 14H_2O$ requires C, 21.35; H, 4.90, N, 18.70; S 9.50%. MS (FAB$^+$ with *m*NBA matrix) *m*/*z* 1097.2 for $[\{Pt(H_3L^1)\}_2 + H]^+$. IR (KBr pellet): ν/cm^{-1} 3161 (w, ^{2}NH), 2925 (s, CH), 1572 (s, CN), 790 (w, CS-thioamide IV band). ^{1}H NMR (100 MHz, DMSO-d_6): δ (ppm) 12.41 (s, ^{2}NH), 3.43 and 3.25 (s, CH_3-thiosemicarbazide), 2.48 (s, CH_3-triazol).

The synthesis of 3,5-diacetyl-1,2,4-triazol bis(4-methyl-thiosemicarbazone) ligand H_5L^2 and its platinum(II) complex $[Pt(\mu\text{-}H_3L^2)]_2$ were carried out as described in references.[24,25] Analytical and spectroscopic properties are consistent with those previously reported.

Crystallography†

A summary of the crystal data, experimental details and refinement results is listed in Table 1. Single crystals were mounted on glass fibers for data collection in a Bruker Kappa APEX II CCD area-detector X-ray diffractometer. X-Ray data were collected at 100 K for H_5L^2 and at 296 K for $[Pt(\mu\text{-}H_1L^1)]_2$. Intensity measurements were collected using graphite-monochromated Mo-Kα radiation ($\lambda = 0.71073$ Å) from a sealed X-ray tube with a monocapillary collimator. The data were collected using 0.5° wide ω-scans and φ-scans, crystal-to-detector distance of 3.5 cm.

The substantial redundancy in data allows semiempirical absorption corrections (SADABS) to be applied using multiple measurements of symmetry-equivalent reflections. The raw intensity data frames were integrated with the SAINT program, which also applied corrections for Lorentz and polarization effects.

The software package SHELXTL version 6.10 was used for space group determination, structure solution and refinement. The structure was solved by direct methods (SHELXS-97), completed with difference Fourier syntheses, and refined with full-matrix least-squares using SHELXL-97 minimizing $\omega(F_0^2 - F_c^2)^2$. Weighted *R* factors (R_w) and all goodness of fit *S* are based on F^2; conventional *R* factors (*R*) are based on *F*. All non-hydrogen atoms were refined with anisotropic displacement parameters. All scattering factors and anomalous dispersions factors are contained in the SHELXTL 6.10 program library.

In vitro antiproliferative activity

The human cancer cells (A2780, A2780cisR and NCI-H460) were grown in RPMI-1640 medium supplemented with 10% foetal bovine serum (FBS) and 2 mM L-glutamine in an atmosphere of 5% CO_2 at 37 °C. Cell proliferation was evaluated by the sulforhodamine B assay. Cells were plated in 96-well sterile plates at a density of 15×10^3 (for NCI-H460) or 4000 (for A2780 and A2780cisR) cells per well with 100 μL of medium and were then incubated for 24 h. After attachment to the culture surface the cells were incubated with various concentrations of the compounds tested freshly dissolved in DMSO (1 mg mL^{-1}) and diluted in the culture medium (DMSO final concentration 1%) for 48 h (for NCI-H460) or 96 h (for A2780 and A2780cisR). The cells were fixed by adding 50 μL of 30% trichloroacetic acid (TCA) per well. The plates were incubated at 4 °C for 1 h and then washed five times with distilled water. The cellular material fixed with TCA was stained with 0.4% sulforhodamine B dissolved in 1% acetic acid for 10 min. Unbound dye was removed by rinsing with 0.1% acetic acid. The protein-bound dye was extracted with 10 mM unbuffered Tris base for determination of optical density (at 515 nm) in a Tecan Ultra Evolution spectrophotometer.

The normal human cells (LLC-PK1) were grown in 199 medium supplemented with 3% foetal bovine serum (FBS) and 1.5 g L^{-1} of sodium bicarbonate in an atmosphere of 5% CO_2 at 37 °C. Cell proliferation was evaluated by the sulforhodamine B assay. Cells were plated in 96-well sterile plates at a density of 10 000 cells per well with 100 μL of medium and were then incubated for 24 h. After attachment to the culture surface the cells were incubated with various concentrations of the compounds tested freshly dissolved in DMSO (1 mg mL^{-1}) and diluted in the culture medium (DMSO final concentration 1%) for 48 h at 37 °C. The cells were fixed by adding 50 μL of 30% trichloroacetic acid (TCA) per well. The plates were incubated at 4 °C for 1 h and then washed five times with distilled water. The cellular material fixed with TCA was stained with 0.4% sulforhodamine B dissolved in 1% acetic acid for 10 min. Unbound dye was removed by rinsing with 0.1% acetic acid. The protein-bound dye was extracted with 10 mM unbuffered Tris base for determination of optical density (at 515 nm) in a Tecan Ultra Evolution spectrophotometer.

The effects of complexes were expressed as corrected percentage inhibition values according to the following equation:

$$\%\text{inhibition} = [1 - (T/C)] \times 100$$

where *T* is the mean absorbance of the treated cells and *C* the mean absorbance in the controls.

The inhibitory potential of compounds was measured by calculating concentration–percentage inhibition curves, these curves were adjusted to the following equation:

$$E = E\text{max}/[1 + (\text{IC}_{50}/C)^n]$$

where *E* is the percentage inhibition observed, E_{max} is the maximal effects, IC_{50} is the concentration that inhibits 50% of maximal growth, *C* is the concentration of compounds tested and *n* is the slope of the semi-logarithmic dose–response sigmoid curves. This non-linear fitting was performed using GraphPad Prism 2.01, 1996 software (GraphPad Software Inc.).

For comparison purposes, the antiproliferative activity of cisplatin was evaluated under the same experimental conditions.

All compounds were tested in two independent studies with triplicate points. These experiments were carried out at the Unidad de Evaluación de Actividades Farmacológicas de Compuestos Químicos (USEF), Universidad de Santiago de Compostela.

Conclusion

The compounds investigated here may be endowed with important antitumor properties, especially H_3L^1 and $[Pt(\mu\text{-}H_3L^2)]_2$ since they are capable of not only circumvent cisplatin resistance in A2780cisR cells but they also exhibit high antiproliferative activity in human non-small cell lung cancer NCI-H460 cells. Moreover, it is important to note that these two compounds exhibit very low nephrotoxicity with respect to cisplatin.

These new compounds with the goal of reducing toxicity while maintaining efficacy stimulate further investigations of thiosemicarbazone compounds and their platinum derivatives, in particular on the spectrum of their antitumour activity as well as on the mechanistic properties.

The studies reported here constitute a good example of how small changes in molecular structure lead to profound differences in biological activity. In our opinion, the conjunction of serendipity and rational design (probability) play a significant role in cancer drug discovery due to the existence of several very specific factors to be considered.

Acknowledgements

We are grateful to Ministerio de Ciencia e Innovación, Instituto de Salud Carlos III (PI080525), Universidad Autónoma de Madrid and Comunidad de Madrid (CCG08-UAM/SAL-4000) of Spain for financial support. C. J. also thanks Erasmus Programme for its Research Placement at Universidad Autónoma de Madrid.

References

1 (*a*) B. Rosenberg, L. Van Camp, J. E. Trosko and V. H. Mansour, *Nature*, 1969, **222**, 385–386; (*b*) J. D. Hoeschele, *Dalton Trans*, 2009, 10648–10650.
2 E. Wong and C. M. Giandomenico, *Chem. Rev.*, 1999, **99**, 2451–2466.
3 Z. Guo and P. J. Sadler, *Angew. Chem., Int. Ed.*, 1999, **38**, 1512–1531.
4 (*a*) M. S. Razzaque, *Nephrol. Dial. Transplant.*, 2007, 1–5; (*b*) M. Okuda, K. Masaki, S. Fukatsu, Y. Hashimoto and K. Inui, *Biochem. Pharmacol.*, 2000, **59**, 195–201.
5 K. von der Schilden, F. García, H. Kooijman, A. L. Spek, J. G. Haasnoot and J. Reedijk, *Angew. Chem., Int. Ed.*, 2004, **43**, 5668–5670.
6 J. M. Pérez, V. Cerrillo, A. I. Matesanz, J. M. Millán, P. Navarro, C. Alonso and P. Souza, *ChemBioChem*, 2001, **2**, 119–123.
7 T. W. Hambley, *Coord. Chem. Rev.*, 1997, **166**, 181–223.
8 J. Kasparkova, V. Marini, Y. Najajreh, D. Gibson and V. Brabec, *Biochemistry*, 2003, **42**, 6321–6332.
9 D. R. Richardson, *Crit. Rev. Oncol. Hematol.*, 2002, **42**, 267–281.
10 D. S. Kalinowski and D. R. Richardson, *Pharmacol. Rev.*, 2005, **57**, 547–583.
11 F. J. Giles, *Leuk. Res.*, 2007, **31**, 1163–1164.
12 E. C. Moore and A. C. Sartorelli, in *Inhibitors of ribonucleotide diphosphate reductase activity*, ed. J. G. Cory and A. H. Cory, Pergamon Press, New York, 1989, pp. 203–215.
13 G. Nocentini, *Crit. Rev. Oncol. Hematol.*, 1996, **22**, 89–126.
14 N. M. F. S. A. Cerqueira, P. A. Fernandes and M. J. Ramos, *Recent Pat. Anti-Cancer Drug Discovery*, 2007, **2**, 11–29.
15 L. Zhu, B. Zhou, X. Chen, H. Jiang, J. Shao and Y. Yen, *Biochem. Pharmacol.*, 2009, **78**, 1178–1185.
16 M. Liu, T. Lin and A. C. Sartorelli, *Prog. Med. Chem.*, 1995, **32**, 1–35.
17 D. X. West, A. E. Liberta, S. B. Padhye, R. C. Chikate, P. B. Sonawane, A. S. Kumbhar and R. G. Yerande, *Coord. Chem. Rev.*, 1993, **123**, 49.
18 A. I. Matesanz and P. Souza, *Mini-Rev. Med. Chem.*, 2009, **9**, 1389–89.
19 C. R. Kowol, R. Berger, R. Eichinger, A. Roller, M. A. Jakupec, P. Schmidt, V. B. Arion and B. K. Keppler, *J. Med. Chem.*, 2007, **50**, 1254–1265.
20 P. Gómez–Saiz, R. Gil-García, M. A. Maestro, J. L. Pizarro, M. I. Arriortua, L. Lezama, T. Rojo, M. González-Álvarez, J. Borrás and J. García-Tojal, *J. Inorg. Biochem.*, 2008, **102**, 1910–1920.
21 R. A. Finch, M. C. Liu, A. H. Cory, J. G. Cory and A. C. Sartorelli, *Adv. Enzyme Regul.*, 1999, **39**, 3–12.
22 R. A. Finch, M. C. Liu, S. P. Grill, W. C. Rose, R. Loomis, K. M. Vasquez, Y. C. Cheng and A. C. Sartorelli, *Biochem. Pharmacol.*, 2000, **59**, 983–991.
23 A. B. Alvero, W. Chen, A. C. Sartorelli, P. Schwartz, T. Rutherford and G. Mor, *Journal of the Society for Gynecologic Investigation*, 2006, **13**, 145–152.
24 A. I. Matesanz and P. Souza, *J. Inorg. Biochem.*, 2007, **101**, 245–253.
25 P. Souza, A. I. Matesanz and C. Pastor, *Inorg. Chem. Commun.*, 2002, **5**, 344–346.
26 V. Suni, M. R. P. Kurup and M. Nethaji, *Spectrochim. Acta, Part A*, 2006, **63**, 174–181.
27 J. S. Casas, A. Castiñeiras, M. C. Rodriguez-Argüelles, A. Sánchez, J. Sordo, A. Vázquez-López and E. M. Vázquez-López, *J. Chem. Soc., Dalton Trans.*, 2000, 2267–2272.
28 U. Abram, K. Ortner, R. Gust and K. Sommer, *J. Chem. Soc., Dalton Trans.*, 2000, 735–744.
29 M. R. Bermejo, A. M. González-Noya, R. M. Pedrido, M. J. Romero and M. Vázquez, *Angew. Chem., Int. Ed.*, 2005, **44**, 4182–4187.
30 L. Papathanasis, M. A. Demertzis, P. N. Yadav, D. Kovala-Demertzi, Ch. Prentjas, A. Castiñeiras, S. Skoulika and D. X. West, *Inorg. Chim. Acta*, 2004, **357**, 4113–4120.
31 D. Kovala-Demertzi, M. A. Demertzis, J. R. Miller, C. Papadopoulou, C. Dodorou and G. Filousis, *J. Inorg. Biochem.*, 2001, **86**, 555–563.
32 P. Souza, A. I. Matesanz and V. Fernández, *J. Chem. Soc., Dalton Trans.*, 1996, 3011–3013.
33 A. I. Matesanz, J. Mosa, I. García, C. Pastor and P. Souza, *Inorg. Chem. Commun.*, 2004, **7**, 756–759.
34 A. I. Matesanz, C. Pastor and P. Souza, *Inorg. Chem. Commun.*, 2007, **10**, 97–100.
35 J. S. Casas, M. S. García-Tasende and J. Sordo, *Coord. Chem. Rev.*, 2000, **209**, 197–261.
36 J. W. Steed, J. L. Atwood, in *Supramolecular Chemistry*, John Wiley & Sons, Chichester, 2nd edn, 2009, ch. 1, pp28-35.
37 J. M. Alonso, M. R. Martin, J. de Mendoza, T. Torres and J. Elguero, *Heterocycles*, 1987, **26**, 989–1000.